4. Diffusion and mixing in microscale

4.1 Diffusion: Principles and applications

4.2 Fast mixing in microscale

4.1.1 Molecular diffusion

Molecular/ionic transport by diffusion is fundamental to natural processes.

Thermodynamics: High to low chemical potential

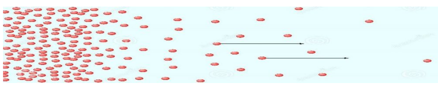

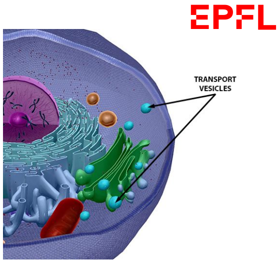

Diffusing vesicles in a cell

Alveolus: oxygen concentration high, carbon dioxide concentration low

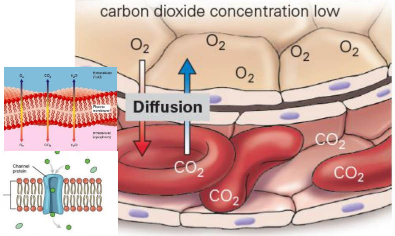

Capillary: oxygen concentration low, carbon dioxide concentration high

Osmosis (red blood cells)
cell membrane ≈ nm

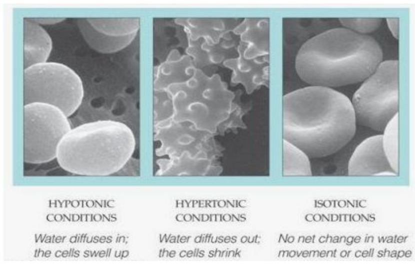

"Microfluidics" -- Thomas Lehnert -- EPFL (Lausanne)

4.1.1 Molecular diffusion: Fast or slow ?

> 10 days

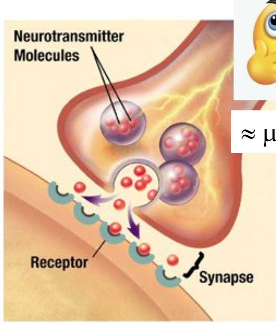

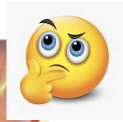

≈ µs range

synaptic cleft ≈ 20 - 40 nm

4.1.1 Molecular diffusion: Fast or slow ?

⇨ A question of scale and particle size …

Diffusion time and length are correlated through the diffusion coefficient of the solute molecule.

$$\boxed{L_0 = \sqrt{DT_0} \quad \text{or} \quad T_0 = \frac{L_0^2}{D}}$$

L_0 diffusion length, T_0 diffusion time,
D diffusion coefficient [m^2/s].

The **diffusion coefficient** depends on **size** and **shape** of the solute molecule, and on interactions with the solvent (viscosity).

$$\boxed{D = \frac{k_{\mathrm{B}}T}{6\pi a\eta}}$$

Einstein relation

⇨ By making length scales small, diffusive timescales may be decreased. *Fast enough for mixing ?*

≈ 1 cm

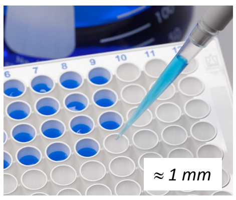

≈ 1 mm

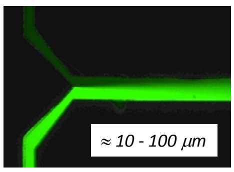

≈ 10 - 100 µm

Diffusion constants and diffusion times


dye

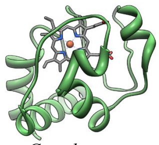
Cytochrome c

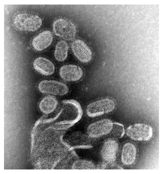
Flu virus

Characteristic diffusivities

Particle	Typical size	Diffusion constant	T_0 (100µm)
Solute ion	10^{-1} nm	2×10^3 μm^2/s	5s
Small protein	5 nm	40 μm^2/s	≈ 4 min
Virus	100 nm	2 μm^2/s	≈ 1h 20 min
Bacterium	1 μm	0.2 μm^2/s	> 2 days
Mammalian/human cell	10 μm	0.02 μm^2/s	> 20 days

$$\boxed{T_0 = \frac{L_0^2}{D}}$$

T.M. Squires et al., Rev. Mod. Phys., Vol. 77, p. 977, 2005

Diffusion time T_0 across a typical microchannel (**width L_0 = 100 µm**)

4.1.2 The passive scalar transport equation

EPFL

Mass current density $\mathbf{J}_\alpha$ for a solute α

$$\mathbf{J}_\alpha \equiv \mathbf{J}_\alpha^{\text{conv}} + \mathbf{J}_\alpha^{\text{diff}} = \rho_\alpha \mathbf{v} + \mathbf{J}_\alpha^{\text{diff}}$$

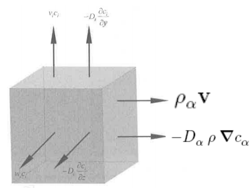

with **Fick's 1st law** (for small gradients) $\boxed{\mathbf{J}_\alpha^{\text{diff}} = -D_\alpha\, \rho\, \nabla c_\alpha}$ (with $\rho_\alpha = \rho\, c_\alpha$)

D_α is the diffusivity of a solute α [m²/s]

⇨ **Convection - diffusion eqn**
(a scalar conservation eqn)

$$\boxed{\partial_t c_\alpha + \mathbf{v}\cdot\nabla c_\alpha = D_\alpha\, \nabla^2 c_\alpha} \qquad (5.22)$$

for v = 0
⇨ **2nd Fick's law for mass diffusion**

$$\boxed{\partial_t c = D\, \nabla^2 c}$$

$$L_0 = \sqrt{DT_0} \quad \text{or} \quad T_0 = \frac{L_0^2}{D}$$

by dimensional analysis

4.1.3 The diffusion equation

EPFL

Equation for mass diffusion (Fick's 2nd law)

$$\boxed{\partial_t c = D\, \nabla^2 c}$$

Limited point-source diffusion: A fixed number of ink molecules is injected in a solution at **r** = 0 and $t = 0$:

$$c(\mathbf{r}, t > 0) = \frac{N_0}{(4\pi D t)^{\frac{3}{2}}}\, \exp\left(-\frac{r^2}{4Dt}\right)$$

(for 3D, normal distributions in x,y,z)

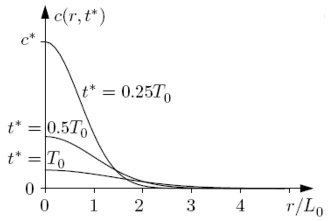

The diffusion length l_{diff} is determined by the variance of (5.35) and increases with dimension (1D, 2D or 3D).

$l^2_{\mathrm{diff,1D}} = 2\,Dt$
$l^2_{\mathrm{diff,2D}} = 4\,Dt$
$l^2_{\mathrm{diff,3D}} = 6\,Dt$

4.1.3 The diffusion equation

EPFL

Equation for mass diffusion (Fick's 2nd law)

$$\boxed{\partial_t c = D\, \nabla^2 c}$$

The transient Stokes eqn is a **momentum diffusion equation** with the **kinematic viscosity** ν as diffusion coefficient

$$\boxed{\partial_t(\rho v_x) = \nu\, \nabla^2(\rho v_x)}$$

$$\nu \equiv \frac{\eta}{\rho} \quad (\approx 10^{-6}\ \mathrm{m^2/s}\ \text{for water})$$

η [Pa s] / ρ [kg/m^3]

4.1.4 Diffusion-based microfluidic devices

Example 1: A microfluidic concept to generate constant diffusion profiles

$$c(x=0,y,z,t>0)=c_0$$

$$c(\mathbf{r},t>0)=c_0\,\mathrm{erfc}\left(\frac{x}{\sqrt{4Dt}}\right) \quad \textit{with} \quad \mathrm{erfc}(s)\equiv\frac{2}{\sqrt{\pi}}\int_s^\infty e^{-u^2}\,\mathrm{d}u \qquad (5.41)$$

Complementary error function

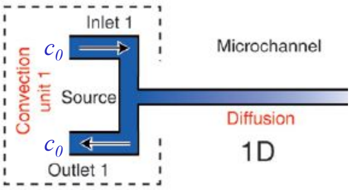

Microfluidic configuration for a constant planar source with matching flow rates at Inlet 1 and Outlet 1.

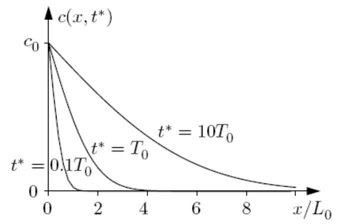

Concentration c(x,t>0) for different t values.*

4.1.4 Diffusion-based microfluidic devices

Example 1: A microfluidic concept to generate constant diffusion profiles

W. Saasi et al., Biomedical Microdevices, Vol. 9, pp 627-635 (2007)

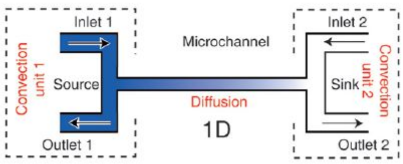

- ⇨ Convection units 1 and 2 act as a perfect source or sink (c_{source} and c_{sink} are const).
- ⇨ The analyte is replenished/removed permanently.
- ⇨ No pressure drop on microchannel, mass transfer only through diffusion.

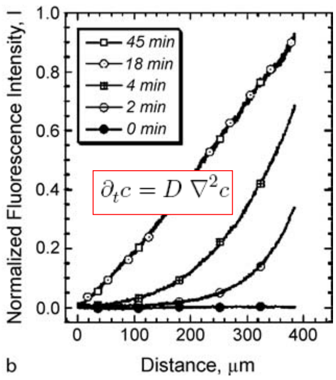

A linear steady-state gradient was established after 18 min.

J. Atencia et al., Lab Chip, 2009, 9, 2707–2714

4.1.4 Diffusion-based microfluidic devices

Example 1: A microfluidic concept to generate constant diffusion profiles

W. Saasi et al., Biomedical Microdevices, Vol. 9, pp 627-635 (2007)

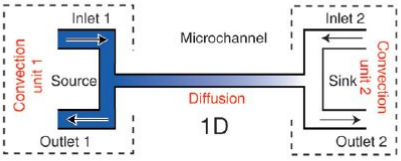

- ⇨ Convection units 1 and 2 act as a perfect source or sink (c_{source} and c_{sink} are const).
- ⇨ The analyte is replenished/removed permanently.
- ⇨ No pressure drop on microchannel, mass transfer only through diffusion.

J. Atencia et al., Lab Chip, 2009, 9, 2707–2714

Microfluidic "ladder" geometry

Main channel height 100 µm, lateral groove height 5 µm): $R_{groove} << R_{main}$

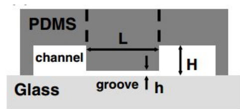

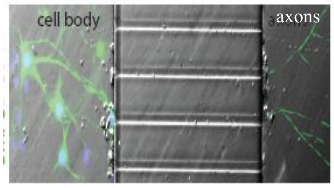

Possible application: gradients of growth factors for axon growth through the microchannels.

4.1.4 Diffusion-based microfluidic devices

Example 2: Protein crystallisation in microfluidic chambers

- ⇨ Obtaining high-quality protein crystals is an outstanding problem in structural biology.
- ⇨ Identification of crystallization conditions requires an empirical search of thousands of chemical conditions.

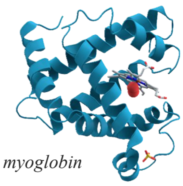

myoglobin

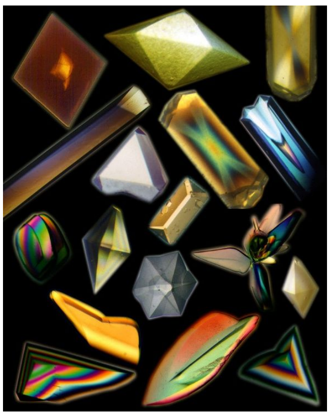

Important parameters:

- **Natural protein solutions** (only milligram quantities available, concentration, purity issues)
- **pH** (buffers such as Tris-HCl)
- **Precipitants** (*e.g.* ammonium sulfate or polyethylene glycol/PEG), and additives
- Temperature

Crystals of proteins and viruses grown on the U.S. Space Shuttle or on Mir. Size range from a few 100 µm in edge length up to more than a millimeter.

en.wikipedia.org/wiki/Protein_crystallization

Example 2: Protein crystallisation in microfluidic chambers

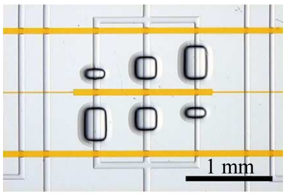

3 compound wells for different mixing ratios of protein solution and precipitation agent.

Separated by valves.

Precise metering: V = 5, 12, 20 nL

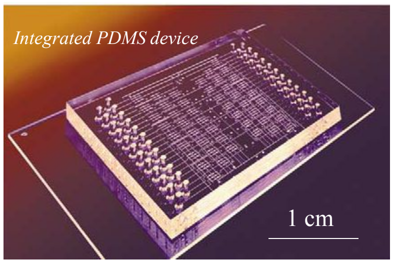

Microfluidic solution

- PDMS/glass chip with reaction chambers separated by valves.
- Highly parallel approach (here 144 reactions)
- Very low sample volumes (nL range)

C. Hansen, et. al, PNAS 2002, 99: 16531–16536
C. Hansen and S. Quake, Current Opinion in Structural Biology 2003, 13:538–544

Example 2: Protein crystallisation in microfluidic chambers

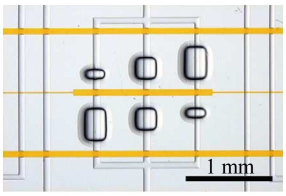

3 compound wells for different mixing ratios of protein solution and precipitation agent.

Separated by valves.

Precise metering: V = 5, 12, 20 nL

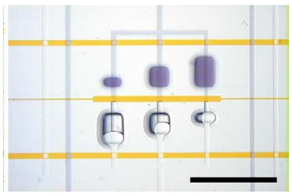

"Dead-end" sample loading of gas permeable PDMS chambers (middle control line closed, bottom line open).

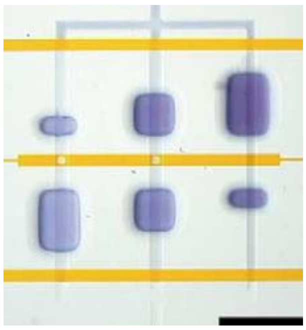

Diffusion and reaction: Interface valves open (middle control line open, others closed).

- Ideally **stable fluidic conditions**
- **Well-defined interface**: High chemical gradients localized in between the chambers.
- **Unique kinetics**: Solvents diffuse "fast" (< 1 h), proteins "slow" (8 to 24 h to equilibrium).

Example 2: Protein crystallisation in microfluidic chambers

EPFL

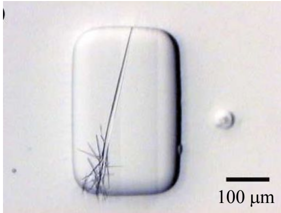

bacterial ***primase***

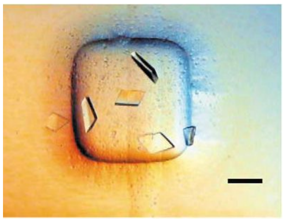

topoisomerase ATPase

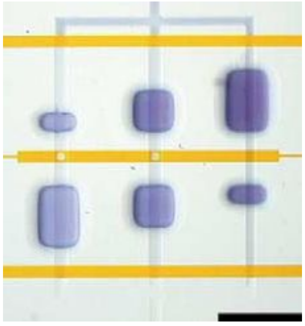

Diffusion and reaction: Interface valves open (middle control line open, others closed).

Growth time is less than 12 hours on a chip (more than 1 week of incubation in conventional setup).

- Ideally **stable fluidic conditions**
- **Well-defined interface**: High chemical gradients localized in between the chambers.
- **Unique kinetics**: Solvents diffuse “fast” (< 1 h), proteins “slow” (8 to 24 h to equilibrium).

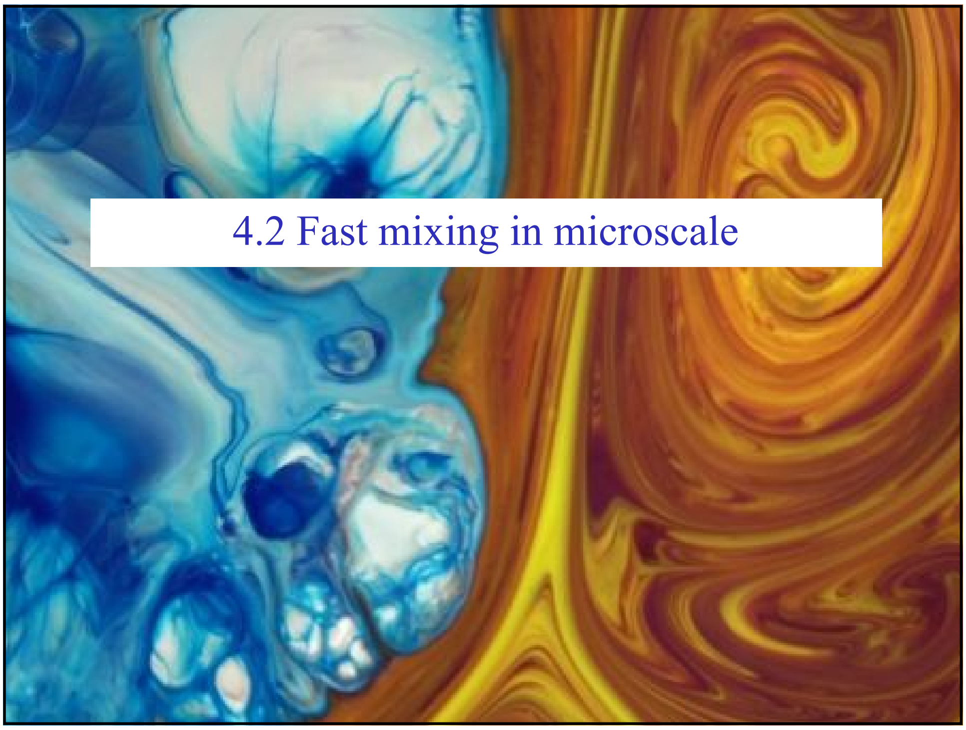

4.2 Fast mixing in microscale

4.2.1 Microfluidic mixing

EPFL

Problems of mixing in microscale at low Re numbers

⇨ Flow is laminar and reversible.

? ⇨ no

⇨ No hydrodynamic instabilities (*e.g.* wakes). Simple flow perturbations do not promote efficient mixing (*e.g.* obstacles in channel).

⇨ Diffusion over the channel width is a generally too slow (especially for larger biomolecules).

⇨ **The ultimate goal is to reduce diffusion length scales !**

See reference list for mixer reviews in the course book !

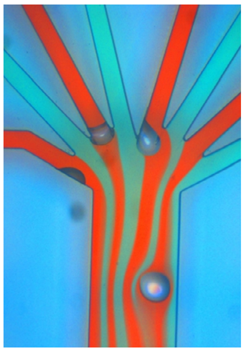

Laminar flow around bubbles

4.2.2 Diffusion mixing *vs.* convection (Péclet number)

EPFL

Example: Two equal solutions are combined in a Y-junction, *e.g.* one contains fluorescent molecules.

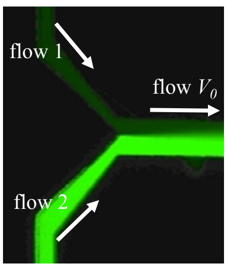

w

How far down the channel ($\boldsymbol{l_{mix}}$) full diffusive mixing will have occurred ?

⇨ uniform concentration profile over w

$\longleftrightarrow$?

l_{mix}

4.2.2 Diffusion mixing *vs.* convection (Péclet number)

Example: Two equal solutions are combined in a Y-junction, one contains **small proteins**.

$D \approx 50\ \mu m^2/s$; $V_0 = 50\ \mu m/s$; $w = 100\ \mu m$

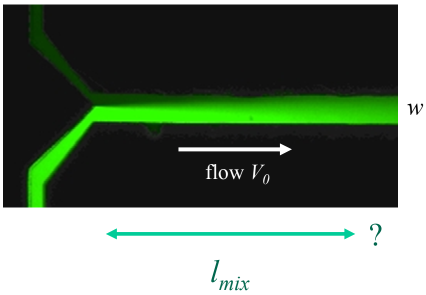

l_{mix} full diffusive mixing will have occurred at…

$\tau_{diff} = w^2/D$ ⇨ $l_{mix} = \tau_{diff} \cdot V_0$

$\tau_{diff} = 200\ s \approx 3\ min$ ⇨ $l_{mix} \approx 1\ cm \approx 100 \cdot w$

Peclét number

$$Pe = l_{mix} / w = V_0 w / D$$

Dimensionless number that defines the ratio of the mixing length to the dimension of lateral diffusion.

4.2.2 Diffusion mixing *vs.* convection (Péclet number)

$$\boxed{Pe \equiv \frac{\text{diffusion time}}{\text{convection time}} = \frac{\tau_{\text{diff}}^{\text{rad}}}{\tau_{\text{conv}}^{a}} = \frac{\frac{a^2}{D}}{\frac{a}{V_0}} = \frac{V_0\, a}{D}}$$

(dimensionless) *tube diameter a*

For a given length scale, e.g. tube diameter or channel width

High *Pe* : Convection dominates

$\tau_{conv} << \tau_{diff}$

Low *Pe* : Diffusion dominates

$\tau_{diff} << \tau_{conv}$

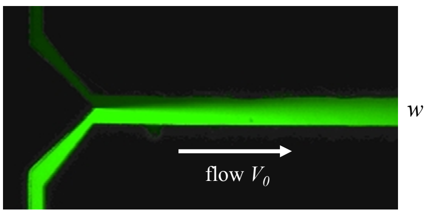

$$\frac{\partial c^*}{\partial t^*} + \vec{u}^* \cdot \nabla^* c^* = \frac{1}{Pe} \nabla^{*2} c^*$$

Pe may be found by dimensional analysis of the convection-diffusion equation.

J. Kirby, *Micro- and nanoscale fluid mechanics*

4.2.2 Diffusion mixing *vs.* convection (Péclet number)

Example: Two equal solutions are combined in a Y-junction, one contains small proteins.

$D \approx 50\ \mu m^2/s$; $V_0 = 50\ \mu m/s$; $w = 100\ \mu m$

$w = a = L_0$

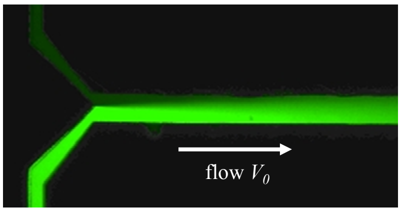

$$\boxed{Pe = \frac{V_0\, a}{D}} \qquad \boxed{Re = \frac{\rho\, V_0\, L_0}{\eta}}$$

***Pe* = 100** ***Re* = 5 x 10^{-3}**

Microfluidic systems normally are operated at high *Pe* numbers (~ up to 10^5) and low *Re* numbers.

⇨ Laminar flow patterning in long channels.

4.2.2 Diffusion mixing *vs.* convection (Péclet number)

Example: Two equal solutions are combined in a Y-junction, one contains small proteins.

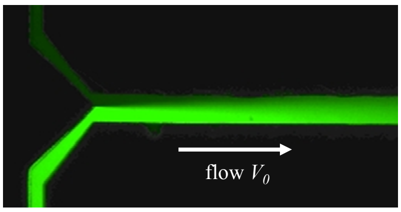

Concentration profile across the channel width

$$\frac{\partial c}{\partial t} = D\frac{\partial^2 c}{\partial x^2}$$

$$c = \frac{1}{2} c_\infty \operatorname{erfc}\left(\frac{x}{2\sqrt{Dt}}\right)$$

Solution for the diffusion eqn: Complementary error function for planar source diffusion.

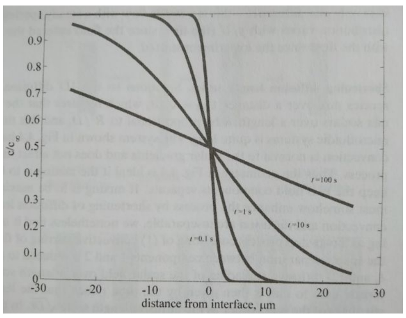

4.2.3 Enhancing diffusion mixing by flow lamination

Example 2: 3D crossing manifold micromixer (CMM)

The "split-and-recombine" strategy:

⇨ Streams to be mixed are divided and reassembled as alternating lamellae.

⇨ (exponential) reduction of interspecies diffusion length and time scales.

Lamination and crossing:

Principle of the horizontally crossing manifold micromixer.

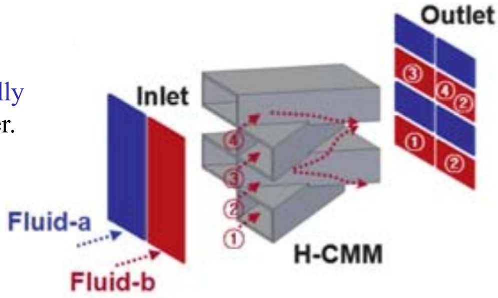

T.W. Lim et al., Lab Chip, 2011, 11, 100–103

4.2.3 Enhancing diffusion mixing by flow lamination

Example 2: 3D crossing manifold micromixer (CMM)

The "split-and-recombine" strategy:

⇨ Streams to be mixed are divided and reassembled as alternating lamellae.

⇨ (exponential) reduction of interspecies diffusion length and time scales.

Lamination and crossing:

Horizontally and vertically crossing manifold micromixers.

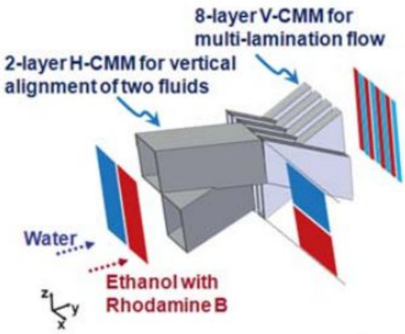

T.W. Lim et al., Lab Chip, 2011, 11, 100–103

4.2.3 Enhancing diffusion mixing by flow lamination

Example 2: 3D crossing manifold micromixer (CMM)

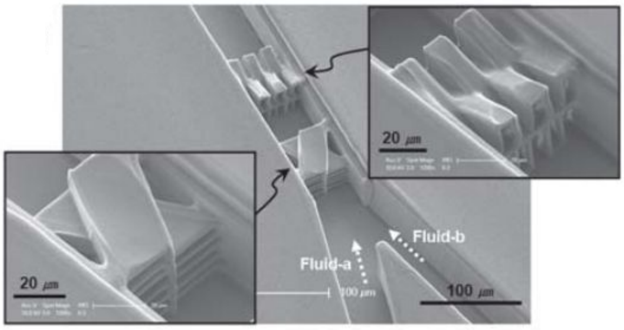

SEM images of the mixers fabricated in the SU8 microchannel by two-photon stereolithography.

T.W. Lim et al., Lab Chip, 2011, 11, 100–103

4.2.3 Enhancing diffusion mixing by flow lamination

Example 2: 3D crossing manifold micromixer (CMM)

Simulation:

Mixing efficiency from H/V-CMM of 2x6 layers. The two fluids are split into 36 segments (Re = 1 and Pe = 1000).

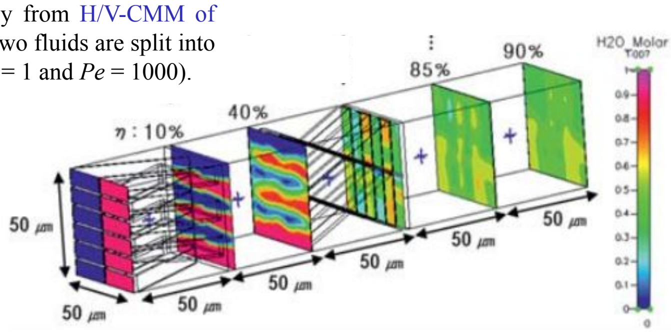

⇨ Almost completely mixed at 5x the channel width (*i.e.* after 200 µm).

⇨ Much better than in a smooth straight channel (mixing length of several millimetres !)

4.2.4 Taylor dispersion and the rotary mixer

Initial condition: A narrow homogeneous band (a plug) of solute(s) is introduce in the channel at $t = 0$ (*e.g.* in high-performance liquid chromatography).

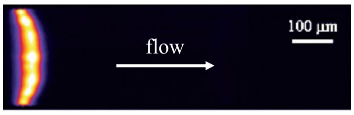

Fluo-dye in a microchannel (250 µm x 70 µm)

The initial concentration gradient is in the axial direction.

4.2.4 Taylor dispersion and the rotary mixer

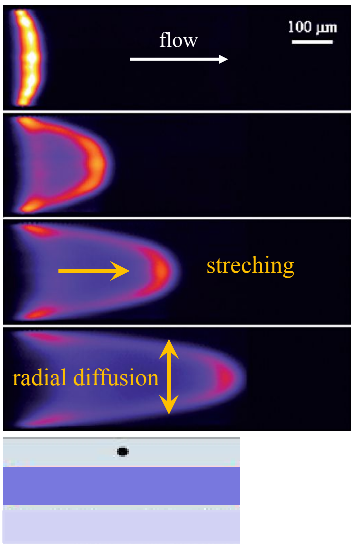

⇨ Upon application of a **steady pressure gradient (Poiseuille flow)**, an initially uniform dye blob is pulled into a parabolic flow "bullet shape".

⇨ Convective stretching creates strong **radial gradients.**

⇨ Diffusion in radial direction tends to homogenize the dye over the channel cross section.

4.2.4 Taylor dispersion and the rotary mixer

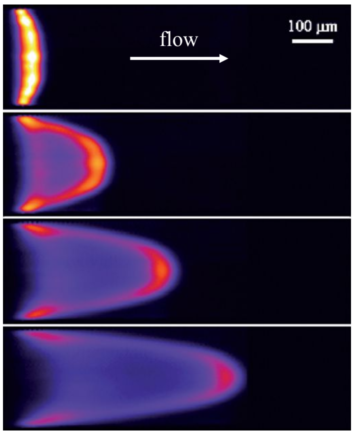

$$D^* \sim D\cdot(1 + K_{geo}\, Pe^2)$$

For high Pe numbers the effective diffusivity D^* increases $\sim Pe^2$ and becomes much higher than the molecular diffusivity D.

for $Pe = 0.1$ $D^* \approx D$

for $Pe = 100$ $D^* \approx 2\cdot 10^{+2}\, D >> D$

⇨ Due to axial dispersion, band broadening occurs with an effective **"Taylor diffusion coefficient" D^***

4.2.4 Taylor dispersion and the rotary mixer

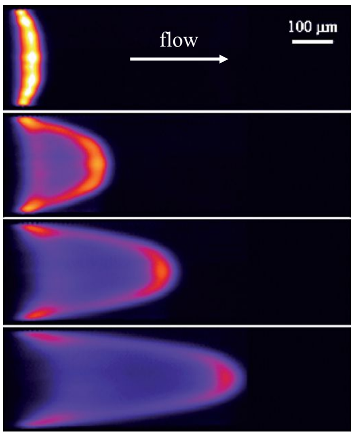

$$D^* \sim D\cdot(1 + K_{geo}\, Pe^2)$$

$$\boxed{D^* = D\left[1 + \frac{1}{48} Pe_d^{\,2}\right]}$$

Cylindrical capillary: diameter d, $Pe_d = U_0 d/D$

$$\boxed{D^* = D\left[1 + \frac{1}{210} Pe_W^{\,2} f\left(\frac{H}{W}\right)\right]}$$

Rectangular channel: width W, height H
$f(H/W)$ is a fct of aspect ratio, $Pe_W = U_0 W/D$

from N.T. Nguyen and S. T. Wereley "*Fundamentals and applications of microfluidics*", Boston: Artech House, 2006

Taylor dispersion derived from the diffusion-convection equation

(for more details see H. Bruus "Theoretical Microfluidics)

Starting with the convection-diffusion eqn (5.22) for a cylindrical microchannel

$$\partial_t c + v_x \partial_x c = D\left(\partial_r^2 c + \tfrac{1}{r}\,\partial_r c + \partial_x^2 c\right) \qquad (5.49)$$

…the 1D convection-diffusion equation for Taylor dispersion can be written

$$\boxed{\partial_t \bar{c} + U_0\,\partial_x \bar{c} = D^*\,\partial_x^2 \bar{c}} \qquad (5.65)$$

for $t \gg \tau_{diff}^{rad}$ (when the dye has diffusively spread over the channel cross-section). $\hat{c}(x,t)$ is the concentration averaged over the cross-section at x, D^* is the Taylor dispersion coefficient and U_0 is the average flow speed. From Fick's law for $\hat{c}(x,t)$ ⇨

$$\boxed{\bar{c}(x,t) = \frac{c_0}{\sqrt{(\pi D^* t)}}\, exp\left[-\frac{(x-U_0 t)^2}{4D^* t}\right]} \qquad (5.67)$$

For $D^* \gg D$: The concentration profile evolves as a Gaussian that moves with U_0 in x-direction and spreads $\sim(D^* \cdot t)^{0.5} = \sim Pe\,(D \cdot t)^{0.5}$.

The rotary mixer

C.L. Hansen et al., PNAS, vol. 101 no. 40 14431–14436 (2004)

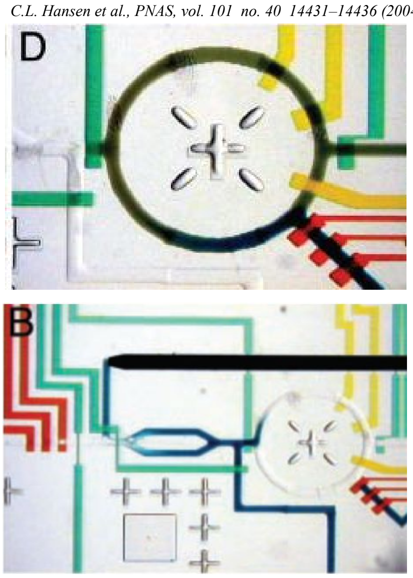

Mixing ring diameter 1.5 mm

5 nL reactor

Arbitrary fluid formulations can be mixed on chip by the sequential injection of **80 pL aliquots**.

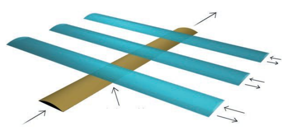

PDMS peristaltic pump with ~ 1-2 nl/s pumping rates (**channels are 100 µm wide and 10 µm high**).

Marc A. Unger, et al., Science 288, 113 (2000)

Microfluidic formulator for combinatorial mixing on chip (video)

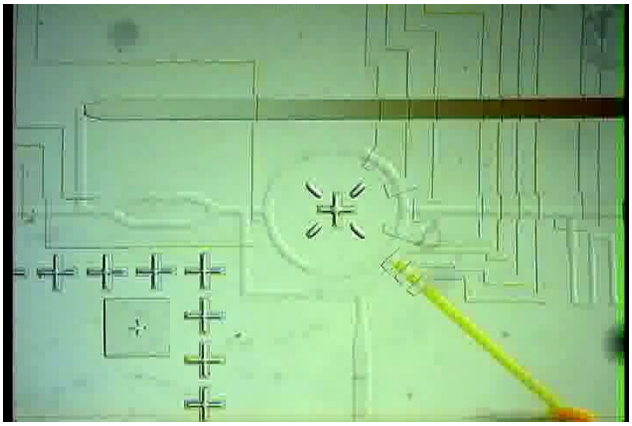

Mixer operation: A separate injection port (yellow) is provided for the combination of a precious sample with a large number of unique chemical formulations. Complete mixing of aqueous reagents was achieved in 3 sec (pumps actuated at 100 Hz, flow velocity 2 cm/sec).

C.L. Hansen et al., PNAS, vol. 101 no. 40 14431–14436 (2004)

How fast mix the fluids in a rotary mixer?

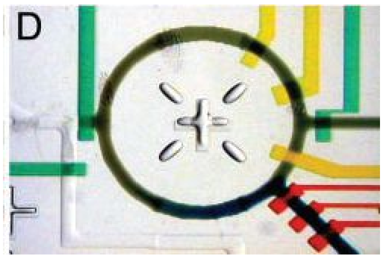

Define the Pe-number for this device

$$Pe = \frac{\tau_D}{\tau_{h,conv}} = \frac{U_0 h}{D} \qquad \text{with} \quad \tau_D \sim h^2/D \quad \text{and} \quad \tau_{h,conv} = h/U_0$$

R ring diameter, h channel width, mean speed U_0

D thermal diffusivity

τ_D diffusion time across the channel width

T. M. Squires and S. R. Quake: Microfluidics: Fluid physics at the nanoliter scale, Rev. Mod. Phys., Vol. 77, p.977, 2005

$$Pe = \frac{\tau_D}{\tau_{h,conv}} = \frac{U_0 h}{D}$$

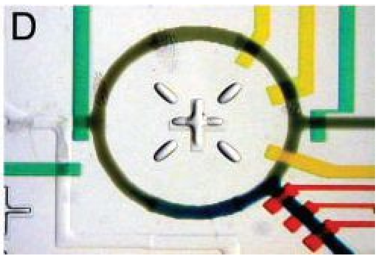

3 mixing regimes (D* Taylor diffusivity)

- ***Diffusion dominated*** (mixing time τ_R)
  $Pe \ll 1$, for $U_0 \rightarrow 0$, $D \approx D^*$
  Basically only thermal diffusion around the ring.
- ***Taylor dispersion mediated*** (mixing time τ_{TD})
  $1 \ll Pe < 2\pi R/h$
  Full diffusion across the channel width occurred before a full convective cycle is completed.
- ***Convective stirring*** (mixing time τ_{con})
  $Pe \gg 2\pi R/h$
  Mixing after multiple cycles before efficient lateral diffusion occurs.

T. M. Squires and S. R. Quake: Microfluidics: Fluid physics at the nanoliter scale, Rev. Mod. Phys., Vol. 77, p.977, 2005

For high Pe number lateral diffusion is very slow compared to convection. Fluidic elements are stretched linearly in time ($\sim U_0$).

The effective distance between branches of the stripe reduces to $h_{eff} \sim h/2N$ **after** N **cycles** (corresponding to a time τ_{con}).

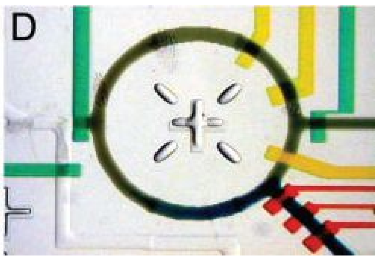

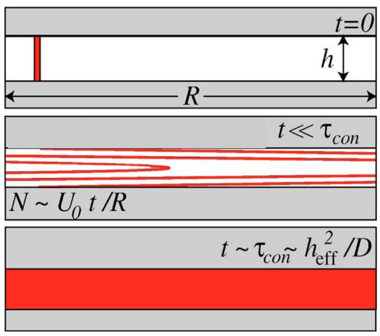

- ***Convective stirring*** (mixing time τ_{con})
  $Pe \gg 2\pi R/h$
  Mixing after multiple cycles before efficient lateral diffusion occurs.

T. M. Squires and S. R. Quake: Microfluidics: Fluid physics at the nanoliter scale, Rev. Mod. Phys., Vol. 77, p.977, 2005

$$Pe = \frac{\tau_D}{\tau_{h,conv}} = \frac{U_0 h}{D}$$

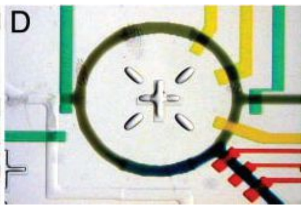

3 mixing regimes

- ***Diffusion dominated*** (mixing time τ_R)
  Pe **<< 1**, for $U_0 \to 0$, $D \approx D^*$
  Basically only thermal diffusion around the ring.

  $\tau_R \approx 200$ **h**
  $Pe = 0$, $U_0 = 0$

- ***Taylor dispersion mediated*** (mixing time τ_{TD})
  1<< ***Pe*** **<** $2\pi R/h$
  Full diffusion across the channel width occurred before a full convective cycle is completed.

  $\tau_{TD} = \tau_D \approx 200$ **s**
  $N_{TD} = 1$ cycle
  $Pe = 60$, $U_0 = 30$ µm/s

- ***Convective stirring*** (mixing time τ_{con})
  Pe **>>** $2\pi R/h$
  Mixing after multiple cycles before efficient lateral diffusion occurs.

  $\tau_{con} \approx 16$ **s**
  $N_{con} = 6.5$ cycles
  $Pe = 10^4$, $U_0 = 5$ mm/s

T. M. Squires and S. R. Quake: Microfluidics: Fluid physics at the nanoliter scale, Rev. Mod. Phys., Vol. 77, p.977, 2005

Protein solubility mapping using microfluidic formulator (video)

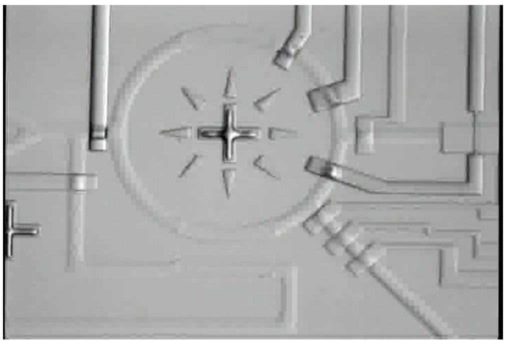

C.L. Hansen et al., PNAS, vol. 101 no. 40 14431–14436 (2004)

Titration of a protein sample (xylanase) into a 5-nL microreactor in which a precipitating solution (1 M potassium phosphate/0.1 M Tris×HCl) has been mixed.

Precipitation of the protein sample is clearly visible and is detected by using image analysis for fully automated protein phase-space mapping.

4.2.5 A multivortex mixer based on inertial flow properties

A.P. Sudarsan and V.M. Ugaz, PNAS, vol. 103(19), 2006, 7228–7233

Mixer based inertial/centrifugal forces (Dean flow) and subsequent flow lamination.
⇨ Flow is injected into a curved channel at relatively high *Re*-number.

Increasing κ ! ⇨ Dean vortices appear !

Dean number κ expresses the relative magnitudes of inertial and centrifugal forces to viscous forces

$$\kappa = \delta^{0.5} Re$$

with $\delta = d/R$

R flow path radius of curvature
d channel hydraulic diameter

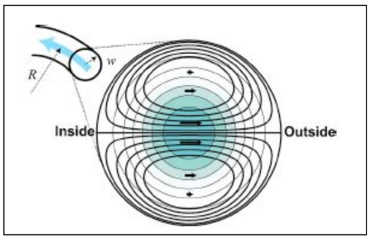

Centrifugal force density is strongest in the center

T. M. Squires et al, 2005, Rev. Mod. Phys., 77, 977-1026

4.2.5 A multivortex mixer based on inertial flow properties

A.P. Sudarsan and V.M. Ugaz, PNAS, vol. 103(19), 2006, 7228–7233

Mixer based inertial/centrifugal forces (Dean flow) and subsequent flow lamination.
⇨ Flow is injected into a curved channel at relatively high *Re*-number.

Dean number κ expresses the relative magnitudes of inertial and centrifugal forces to viscous forces

$$\kappa = \delta^{0.5} Re$$

with $\delta = d/R$

R flow path radius of curvature
d channel hydraulic diameter

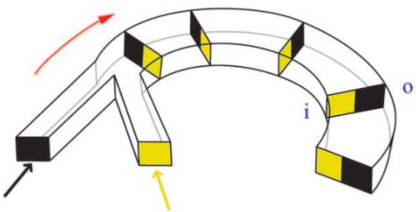

4.2.5 A multivortex mixer based on inertial flow properties

A.P. Sudarsan and V.M. Ugaz, PNAS, vol. 103(19), 2006, 7228–7233

Mixer based inertial/centrifugal forces (Dean flow) and subsequent flow lamination.
⇨ Flow is injected into a curved channel at relatively high *Re*-number.

Dean number κ expresses the relative magnitudes of inertial and centrifugal forces to viscous forces

$$\kappa = \delta^{0.5} Re$$

with $\delta = d/R$

R flow path radius of curvature
d channel hydraulic diameter

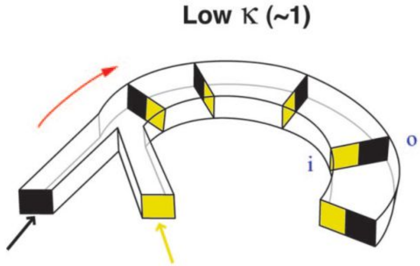

*Laminar flow pattern at low **Re** and κ*
No mixing !

4.2.5 A multivortex mixer based on inertial flow properties

A.P. Sudarsan and V.M. Ugaz, PNAS, vol. 103(19), 2006, 7228–7233

Mixer based inertial/centrifugal forces (Dean flow) and subsequent flow lamination.
⇨ Flow is injected into a curved channel at relatively high *Re*-number.

How can mixing be achieved with this device ?

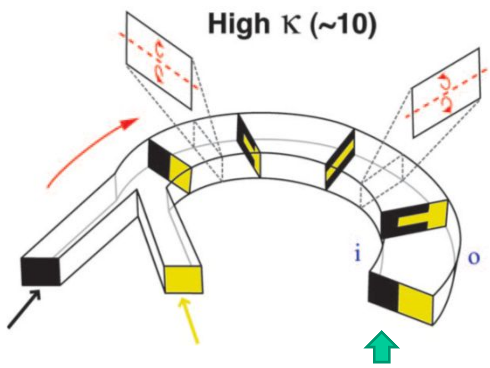

Inverted flow pattern due to Dean vortices
No mixing !

4.2.5 A multivortex mixer based on inertial flow properties

A.P. Sudarsan and V.M. Ugaz, PNAS, vol. 103(19), 2006, 7228–7233

Mixer based inertial/centrifugal forces (Dean flow) and subsequent flow lamination.

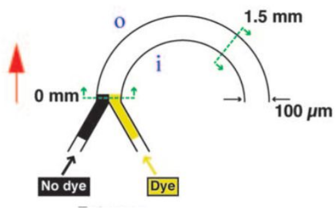

Dean flow pattern
1.5 mm downstream

$2.6 \leq Re \leq 45.1$ $(0.7 \leq \kappa \leq 12.1)$

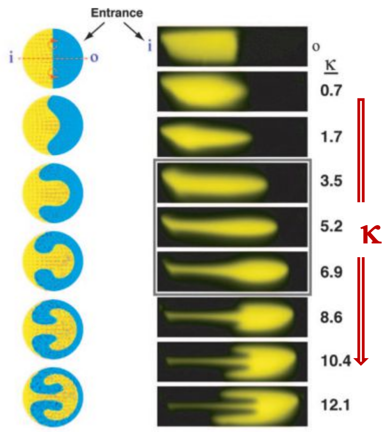

Mixer based inertial/centrifugal forces (Dean flow) and subsequent flow lamination.

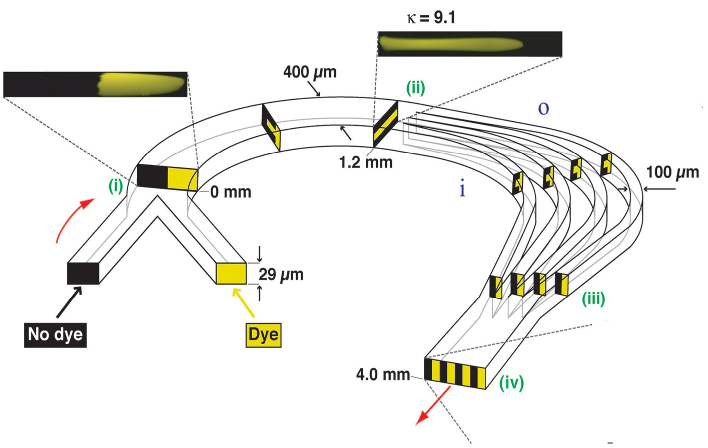

(i) Parallel streams experience a transverse flow generated by the counterrotating vortices.

(ii) The flow is split into 4 parallel streams inducing fluid rotations in each stream.

Between *(ii)* and *(iii)* Alternating lamellae of the two species are generated when the streams are rejoined 4 mm downstream from the entrance ***(iv)*.**

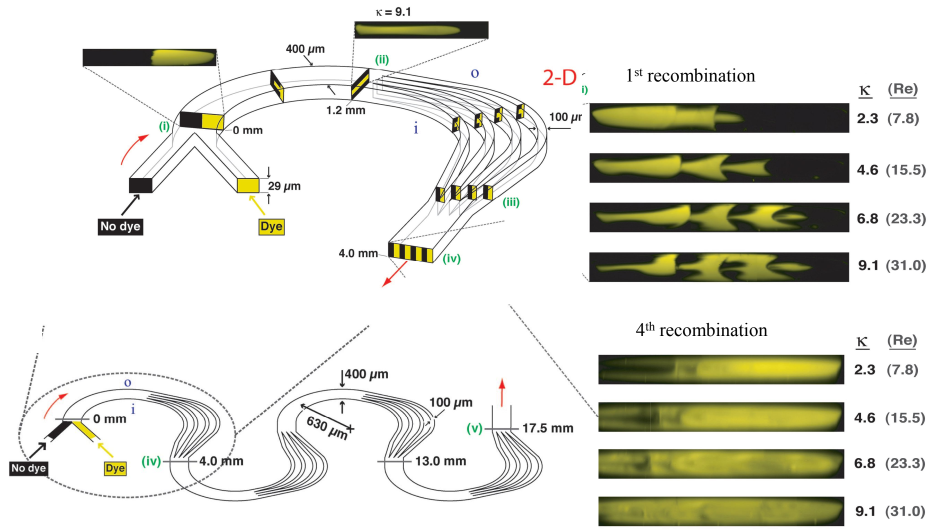

Microchannel incorporating a series of successive mixing elements.

4.2.6 Mixing based on chaotic advection

Butterfly effect

not chaotic !

chaotic !

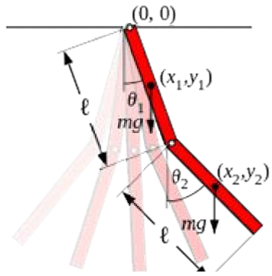

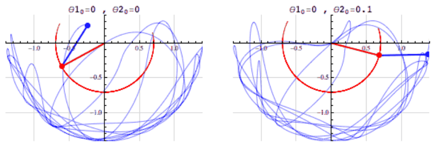

The motion of a **double pendulum** is governed by a set of coupled ordinary differential equations and is chaotic (deterministic, not random).

https://en.wikipedia.org/wiki/Butterfly_effect

4.2.6 Mixing based on chaotic advection

A dynamic system is ***chaotic* if the trajectories of two points (here fluidic elements) diverge exponentially**.

$$\boxed{\delta x(t) \approx \delta x_0\, e^{\alpha t}}$$

δx_0 initial distance of two particles
δx is the distance at time t

chaotic if $\alpha > 0$

Lyapunov number α defines the rate of exponential divergence in a chaotic system.

⇨ Chaotic systems are extremely sensitive to initial conditions.

⇨ Experimentally, the initial conditions cannot be defined accurately enough (*e.g.* $\delta x_0 \pm \delta x_B$ due to Brownian motion) to predict a particle's position after a certain time $t > 0$.

Is it possible to create chaotic particle trajectories in a laminar flow system ?

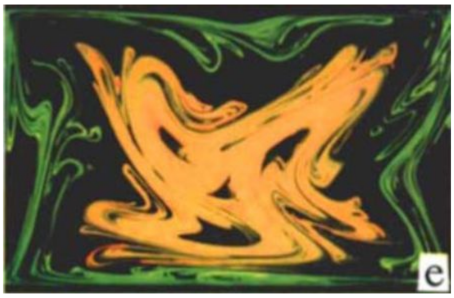

J. M. Ottino, 1989, *The Kinematics of Mixing: Stretching, Chaos, and Transport,* Cambridge University Press, Cambridge, England.

Chaotic particle trajectories in laminar flow regimes

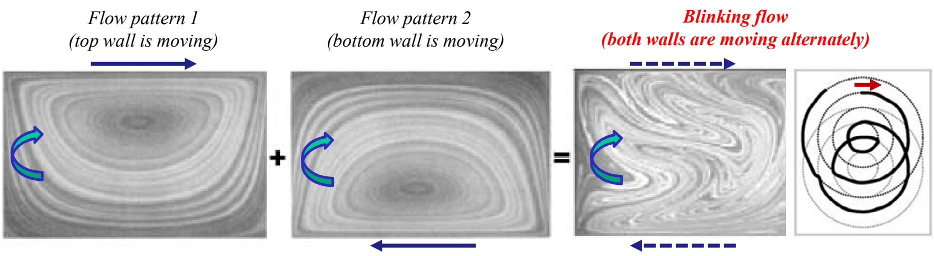

Picture on the right:

Periodically changing boundary conditions (both walls move alternately), resulting in chaotic and diverging dye trajectories (whereas the streamlines of the flow are well-defined !).

⇨ Very thin striations, high local gradients and exponential decrease of the interface distances may significantly increase diffusive mixing.

J. M. Ottino, 1989, *The Kinematics of Mixing: Stretching, Chaos, and Transport,* Cambridge University Press, Cambridge, England.

The baker's transformation and chaotic mixing

The baker's transformation and chaotic mixing

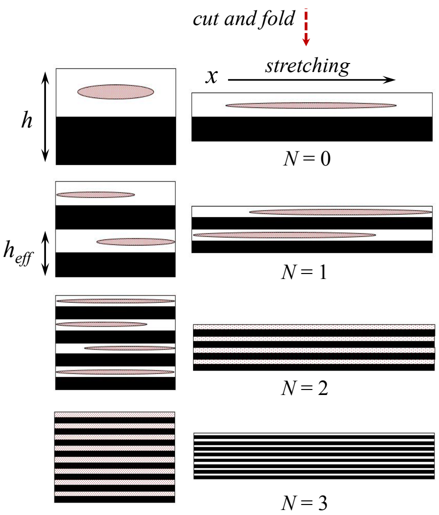

***Baker's Transformation*:**

***N* cycles of repeated stretching and folding** (or cutting and piling up as shown here).

The distance in x direction of two arbitrary points in a layer increases as

$$\delta x(t) \approx \delta x_0\, 2^N \sim e^{N\,\ln 2}$$

A baker's transformation generates deterministic chaos with a Lyapunov exponent $\alpha = \ln 2$.

The effective diffusion length (spacing between two layers) decreases exponentially with N

$$h_{eff} = \frac{h}{2^N} \sim e^{-N}$$

The baker's transformation and chaotic mixing

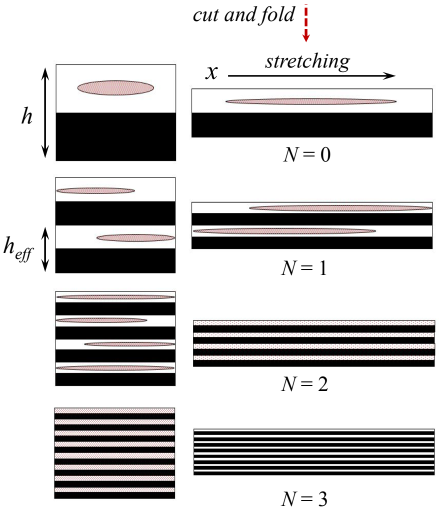

A chaotic microfluidic mixer based on Baker's transformation is built up from N units that perform successive stretching/folding processes in a continuous flow mode.

$$\boxed{L_{\mathrm{mix}} = N_{\mathrm{chaotic}} \cdot L_{\mathrm{cyc}} \sim \ln Pe}$$

For comparison:

Diffusion-based mixing in a linear channel

$$L_{mix} \sim Pe \,!$$

Example 1: Topologic mixing on a microfluidic chip

H. Chen, et al., Applied Physics Letters, 2004, Vol. 84, 2193–2195

The structure exploits laminarity to repeatedly fold and stretch the flow. Lamination doubles the lateral concentration gradient after each cycle and increases the interfacial area $\sim 2^N$.

The distance between the layers is reduced as $h_{eff} \sim h/2^N$ **after** N **cycles**.

The mixer performs a series of Baker's transformations on the concentration profile.

⇨ **Chaotic advection**

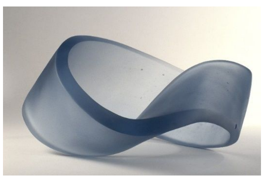

A Möbius band-like fluidic flow pattern is generated.

Two identical streams are split and rotated in opposite directions in each channel (width 100 µm). Upon recombination the concentration pattern and gradients are doubled.

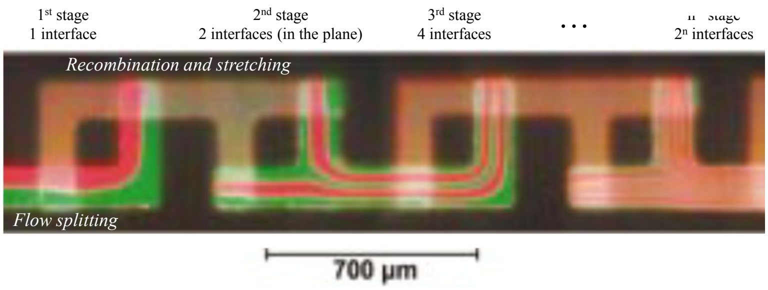

Mixing of two fluorescently labeled protein solutions resulting in mixing after 4-5 stages (2-3 mm). After the first two mixing stages, four interfaces, now broadened by diffusion, are visible.

***Experimental result*: The unmixed volume indeed decreases exponentially with the number of mixing stages.**

$$\boxed{L_{mix} = N_{stages} \cdot L_{cyc} \sim \ln Pe}$$

Example 2: Staggered herringbone mixer (SHM)

EPFL

A.D. Strook et al., Science, 295, p.647 (2002)

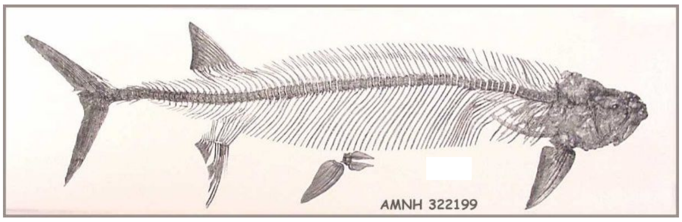

Passive mixing of steady pressure-driven flows based on chaotic advection in microchannels.

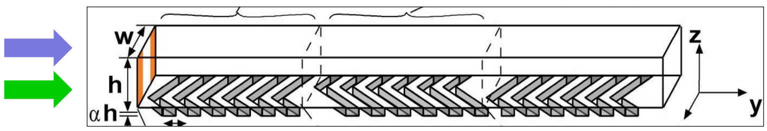

What happens to the injected flow ?

Example 2: Staggered herringbone mixer (SHM)

A.D. Strook et al., Science, 295, p.647 (2002)

A) PDMS channel with obliquely oriented ridges on the bottom.

Secondary transverse flow resulting in 3D twisting trajectories.

Helical streamlines in the (x,z) cross section are shown.

B) Top view of a red and a green stream flowing on either side of a clear central stream at the inlet.

C) Fluorescent confocal micrographs of vertical (x,z) cross sections of the microchannel.

Rotation, distortion and stretching of a fluidic volume element that was injected along one side.

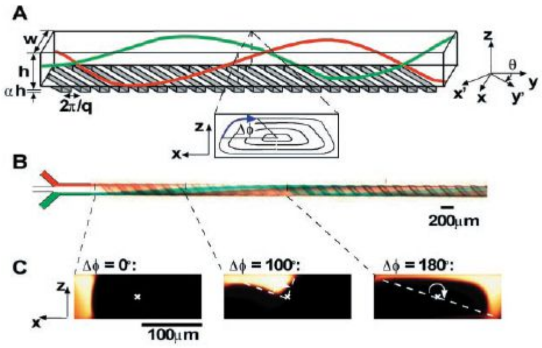

Channel (h = 70 μm, w = 200 μm)

Staggered herringbone structure

Changing the asymmetry of the herringbone structure after each half-cycle shifts the center of rotation of both secondary flows. Two counter-rotating transverse flows are generated.

⇒ Baker's transformation ("blinking flow") with repeated folding and stretching of the transverse flows.

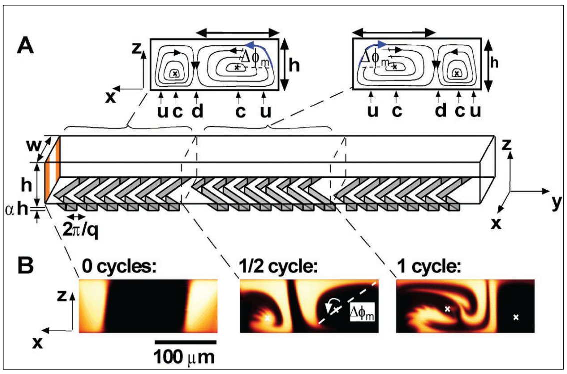

(A) One-and-a-half cycles of the SHM: One mixing cycle is composed of two sequential regions of ridges with different directions of asymmetry. The streamlines are shown.

(B) Confocal micrographs cross sections. Two fluorescent solutions were injected on either side of a clear central stream.

A.D. Strook et al., Science, 295, p.647 (2002)

Mixing performance of different channel configurations

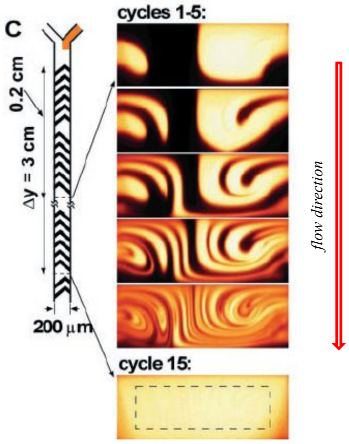

SHM, *Pe* = 9×10⁵ (!) ⇨ full mixing

The distance between two stripes, *i.e.* the effective diffusion length, decreases ~2^{-N} after *N* cycles.

length Δy = 3 cm, w = 200 µm, h = 80 µm

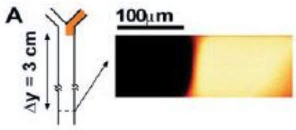

smooth channel walls

$Pe = 2\times10^5$, no mixing

***Example:* Mixing of a proteins in aqueous solution**

$D \approx 10^{-6}$ cm²/s , w = 100 µm

with	**U_0 = 10 cm/s, $Pe = 10^5$**
Smooth walls	Δy_m ~ 10 m (!)
SHM	Δy_m ~ 1.5 cm